Journal of Sol-Gel Science and Technology (2023) 108:742–755
https://doi.org/10.1007/s10971-023-06223-6

ORIGINAL PAPER

The role of TiO_2 nanoparticles in enhancing the structural, optical, and electrical properties of PVA/PVP/CMC ternary polymer blend: nanocomposites for capacitive energy storage

Mohammed M. Damoom[1,2] · Abdu Saeed[3,4] · Eida M. Alshammari[5] · Abdulsalam M. Alhawsawi[1,2] · A. Y. Yassin[6] · J. A. Mohammed Abdulwahed[7] · A. A. Al-Muntaser[8]

Received: 22 July 2023 / Accepted: 30 August 2023 / Published online: 19 September 2023

Abstract

Herein, titanium dioxide (TiO_2) nanoparticles (NPs) were prepared via the sol–gel technique; then, they were incorporated into a ternary blend polymer matrix to design polymer nanocomposite (PNC) films through the solution casting technique. The ternary blend polymer matrix consisted of polyvinyl alcohol (PVA), polyvinyl pyrrolidone (PVP), and carboxymethyl cellulose (CMC). X-ray diffraction (XRD) analysis revealed reductions in the crystallinity structure of the polymer matrix after adding TiO_2 NPs. The optical study manifested increases in the refractive index and reduction in the optical bandgap values, which reduced from 4.97 eV for the pure polymer blend to 4.77 eV for the PNC film at TiO_2 content of 3 wt%. Additionally, the transmission edge gradually shifted towards lower energy. The PNC films exhibited considerable improvements in the dielectric constant (ε'), dielectric loss (ε''), dielectric moduli (M' and M''), and electrical conductivity characteristics over the range of frequency range from 0.1 Hz to 10 MHz. The addition of TiO_2 NPs improved the electrical conductivity and dielectric constant significantly. The electrical conductivity increased by over ten times compared to the pure ternary polymer blend, and ε' also rose four-fold at 100 Hz. The enhancement in the electrical and dielectric parameters of the PNC films after adding TiO_2 nanofiller could indicate the suitability of these samples for flexible-type energy storage applications, such as dielectric capacitors.

Graphical Abstract

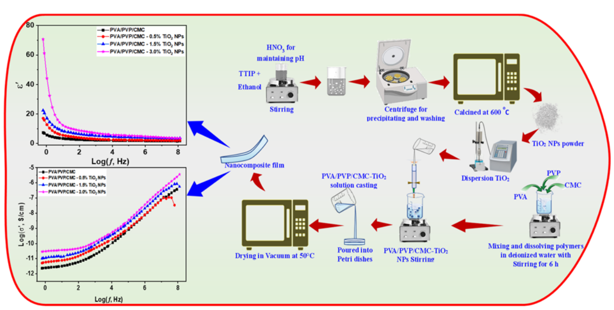

Keywords TiO_2 NPs · Sol–gel · Polymers · Nanocomposite · Energy storge

✉ Abdu Saeed
Abdusaeed@tu.edu.ye

✉ A. A. Al-Muntaser
almuntser2015@gmail.com

Extended author information available on the last page of the article

Highlights

- TiO_2-NPs were prepared via sol–gel technique.
- TiO_2-NPs were used as a nanofiller with PVA/PVP/CMC blend to prepare nanocomposites.
- The FTIR and XRD indicated the interaction between the polymer blend and TiO_2-NPs.
- The band gap of PVA/PVP/CMC blend decreased with increasing TiO_2-NPs content.
- The electrical and dielectric results show the use of the samples in energy storage.

1 Introduction

Integrating nano-sized components into polymer blends creates nanocomposites with superior properties compared to micro- and macro-composites [1, 2]. The nanocomposite blended polymer's organic and inorganic material features have positioned it for use in a wide range of technical applications, including transistors for electrical switches, solar photovoltaic cells, and the electrode of energy storage [1, 3]. Compared to pure polymers and conventional composites, the metal oxides based nanocomposites display considerable advantages in mechanical, thermal, and barrier properties, allowing them to serve as a source of high-performance new materials with several new applications [4–12].

Using the polymer blend technique can enhance the amorphous phases of a semicrystalline polymer [13]. Several polymers have been utilized to prepare solid polymer blends, such as chitosan (CH)/methylcellulose (MC) [14], polyethylene oxide (PEO)/carboxymethyl cellulose [7], PVA/sodium alginate (SA) [8], PEO/MC [13], PEO/ polyvinyl pyrrolidone (PVP) [9], and CH/PVA [15]. These prepared polymer blends exhibited enhanced electrical and dielectric properties compared to their pristine polymers.

PVA is a polymer with hydroxyl groups linked to a carbon derived from methane and has several characteristics, including excellent transparency, flexibility, and nontoxicity. PVP polymer possesses both hydrophobic and hydrophilic functional groups, making it soluble in a variety of solvents and water. CMC, which is a cellulose derivative, is used in the food, cosmetic, and pharmaceutical sectors. Furthermore, CMC has good film-forming characteristics, which results in transparent coatings [16].

Nanoparticles (NPs) incorporation into the matrix of synthetic and polymer films is one of the most successful ways to improve them. Titanium dioxide (TiO_2) is a highly promising material that has been incorporated with different materials [8, 17–25] due to its many desirable qualities. It is chemically stable, transparent in the visible range, has a high dielectric constant, is nontoxic, has a low unit cost, and has a large band gap. It is extensively used in many applications, including but not limited to photoelectrochemistry [18], dye-sensitized solar cells [17], electrochromic devices [19], gas sensing [20], lithium-ion batteries anode [23], catalysis [24, 26], waveguide applications [25], and other applications with polymers [8, 21]. Additionally, TiO_2 is a potential material for replacing carbon-based anodes in lithium-ion batteries [27]. TiO_2 NPs are also well-known for their many benefits, such as their high photocatalytic activity, hydrophilic qualities, UV blocking ability, an increase of certain physicochemical features, ability to strengthen nanocomposites, and antibacterial capacity [28].

Several efforts [6, 8, 29–31] have been performed in recent years on the production of polymer nanocomposite (PNC) films by combining various polymers with TiO_2 NPs. By incorporating TiO_2, Ren et al. [29] improved the mechanical performance of PVA/xylan composite films. According to Bisen et al. [30], PVA with minimal doping is ideal for transmitting desired properties without causing bond ruptures in the polymer host. PNCs that use a blend of PVP and CMC, along with hybrid NPs made from multi-walled carbon nanotubes and silver, were prepared and found appropriate for an assortment of applications, including optoelectronics and nanodielectrics [32].

Despite the aforementioned efforts, there is still a need for functional materials with excellent dielectric properties, low cost, and ease of preparation for energy storage applications. Herein, extensive research was conducted on the TiO_2 NPs prepared via the sol-gel route; then, they were used to design PVA/PVP/CMC of PNC films, analyzing their crystallinity and chemical functional groups through X-ray diffraction (XRD) and Fourier-transform infrared spectroscopy (FTIR), respectively. Additionally, their optical and morphological properties were thoroughly examined using UV–Vis and transmission electron microscope (TEM), respectively. Moreover, the conduction mechanisms of these samples were also investigated and systematically interpreted.

2 Experimental work

2.1 Materials

The polymers used in this work are PVA and CMC powder (BDH Chemicals Ltd Poole, UK) and PVP (SISCO Research Laboratory Ltd, India) powder with Mw of 14000,

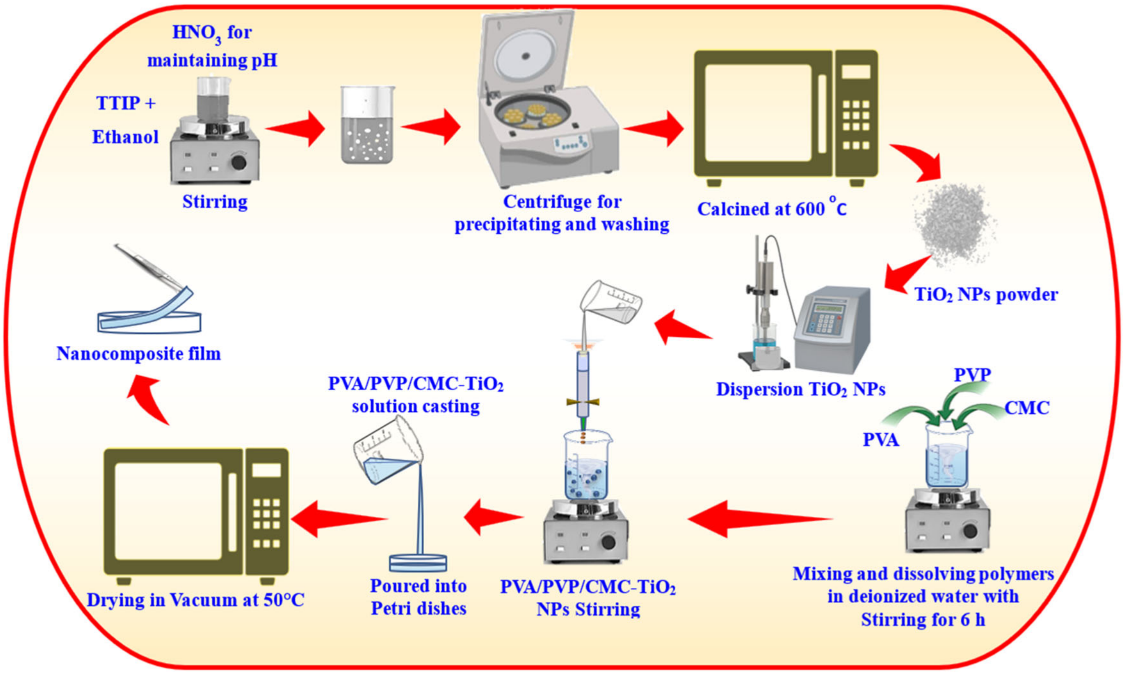

Scheme 1 A diagram illustrating the process of preparing TiO_2 nanoparticles and PNC films

250,000, and 72,000 g/mol, respectively. Also, titanium isopropoxide [$C_{12}H_{28}O_4Ti$] with a purity of 99%, nitric acid [HNO_3], and ethanol from (Sigma-Aldrich, Germany) were used during TiO_2 NPs preparation. Deionized water was for washing and during the preparation.

2.2 TiO_2 NPs and nanocomposites preparation

Per the previous study [26], TiO_2 NPs were prepared via the sol-gel technique with necessary modification and utilized as an inorganic nanofiller to prepare PVA/PVP/CMC/TiO_2 nanocomposites. Three hours were spent calcining the TiO_2 powder at 600 °C. The obtained TiO_2 NPs were then used to fabricate the PVA/PVP/CMC/TiO_2 PNC films via the solution casting process. A 120 ml of deionized water was used to dissolve (1.225 g PVA + 0.735 g PVP + 0.49 g CMC) to create the blend solution of the PVA/PVP/CMC (50/30/20 wt%). Then, the TiO_2 nanofiller was mixed into the blend solution at varied filling levels of 0.5 and 1.5, and 3.0 wt% while being stirred at 50 °C. Then, we produced the PNC of PVA/PVP/CMC-TiO_2 solutions and cast them into glass Petri plates before drying them at 50 °C. The thicknesses of the prepared PNC films range from (0.004–0.005 cm). Scheme 1 summarizes the process of preparation of TiO_2 NPs and PNC films.

2.3 Characterization

We utilized the XRD model X'Pert PRO (Malvern PANalytical, USA) to analyze the crystal structures of the nanofiller and nanocomposite PNC films. The examination was conducted within the 3–80° range using a CuK source with a wavelength of 1.5418 Å. To obtain the FTIR spectra for the PNC films, we utilized an FTIR spectrometer, model Nicolet iS10 (Thermo Scientific, USA). Additionally, we used TEM, model JEM-2100 (JEOL, Japan), to measure the size and shape of the TiO_2 NPs. We utilized a spectrophotometer, model V-570-UV–VIS-NIR (JASCO, Japan), to measure transmittance spectra with a precision of 0.2 nm, between 190 and 2500 nm. The PVA/PVP/CMC-TiO_2 PNC films' electrical conductivity and dielectric characteristics were conducted at room temperature in a dry nitrogen atmosphere using model Concept 40 (Novocontrol Technologies, Germany). The cell that was used for electrical and dielectric measurements is a three-terminal electrode (three electrodes, i.e., top, bottom, and guard electrodes), and the applied Vrms voltage is 1 V.

3 Results and discussion

3.1 XRD analysis

XRD investigations play a crucial role in understanding microstructural changes in polymeric materials. In this regard, we utilized XRD to determine whether the PVA/PVP/CMC-TiO_2 NPs PNC films had amorphous or crystalline areas and evaluate how TiO_2 NPs affected the PNCs' structural properties.

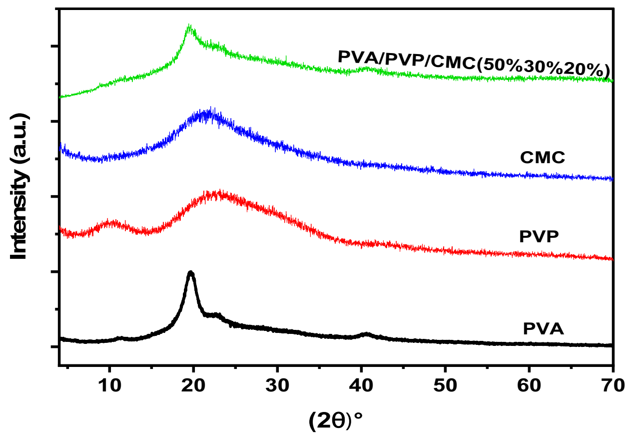

Fig. 1 XRD patterns of the PVA, PVP, CMC, and PVA/PVP/CMC ternary blend

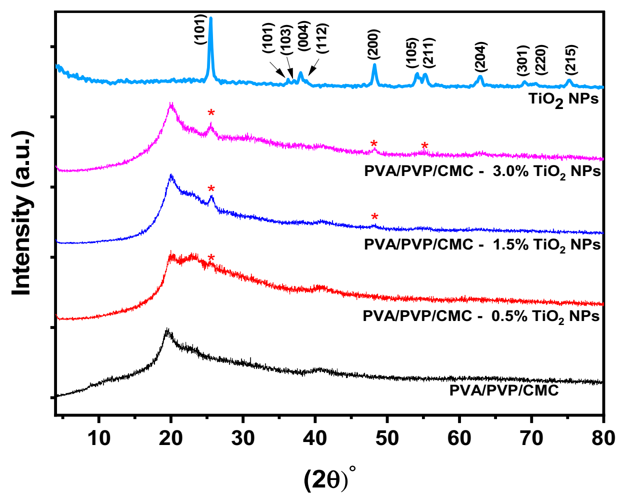

Fig. 2 XRD patterns of the PVA/PVP/CMC ternary blend and the PNCs filled with TiO_2 NPs contents of 0.5, 1.5, and 3 wt%

XRD patterns for the PVA, PVP, CMC, and PVA/PVP/CMC ternary blend are exhibited in Fig. 1. The PVA/PVP/CMC ternary blend is characterized by a broad peak centered at $2\theta \approx 19.52°$, which is attributed to the semicrystalline nature of the PVA with (101) reflective plane [33, 34]. The evident broadness in this main peak confirms the semicrystalline nature of the current ternary blend.

XRD patterns of the ternary polymers blend filled with TiO_2 NPs contents of 0.5, 1.5, and 3 wt% are illustrated in Fig. 2. In the XRD patterns of the prepared nanocomposites, with the addition of TiO_2 NPs, it can be observed a little increase in the broadening of the broad peak (shadowed by green) seen in the pure PVA/PVP/CMC blend, suggesting decreasing in crystalline ratios in the PVA/PVP/CMC blend matrix. Besides, there is a shift, in the position of the same broad peak, towards a higher angular angle. Moreover, new sharp diffraction peaks were observed at $2\theta = 25.52°$, 48.24°, and 55.28°; based on the XRD standard card (JCPDS file No. 21-1272), these diffracted peaks were attributed respectively to (101), (200), and (211) atomic plane in the TiO_2 crystal structure, confirming the successful synthesis of the tetragonal anatase phase of TiO_2 NPs [35]. The intensity of these peaks also increased with the rise in nanofiller contents, indicating the effective complexation and compatibility of the TiO_2 NPs with the ternary blend host material. It appears that the TiO_2 NPs have integrated well with the blend matrix. Upon comparing the XRD of pure TiO_2 and PNCs filled with TiO_2 NPs at 0.5, 1.5, and 3 wt%, some diffraction peaks corresponding to the lattice planes of pure TiO_2 were not observed in the PNCs. This result could be due to two reasons: the low TiO_2 content (maximum 3%) or the TiO_2 nanofillers wrapped inside the polymer blend matrix.

Table 1 The calculated value of crystalline degree (X_{dc} %), indirect/direct energy gap (E_g), and refractive index (n) for the present films

Sample	X_{dc} %	E_g (eV)		n
		Direct	Indirect	
Pure PVA/PVP/CMC	23.03	5.43	4.97	2.00
PVA/PVP/CMC −0.5%Ti NPs	21.62	5.39	4.91	2.01
PVA/PVP/CMC −1.5%Ti NPs	17.77	5.27	4.72	2.04
PVA/PVP/CMC −3.0%Ti NPs	13.01	5.34	4.77	2.04

The Scherrer equation was employed to determine the average crystallite size, which involves the use of the following formula:

$$X_w = \frac{0.94\,\lambda_i}{D_c \cos\theta_m} \quad (1)$$

where, θ_m is Bragg's angle, X_w represents the full width at half maximum of the diffraction peak, and λ is the X-ray wavelength of the XRD machine ($\lambda_i = 0.154056$ nm). The calculated D_c value of TiO_2 NPs is 12.42 nm. The diffraction peaks in the PNC films' XRD patterns were attributed to PVA, PVP, CMC, and TiO_2 NPs. The crystallinity degree (X_{dc} %) was determined using the Hermans-Weidinger method [36]:

$$X_{dc} = \frac{(\text{area under crystalline peaks})}{(\text{the total area under all peaks})} \times 100 \quad (2)$$

Table 1 shows the calculated X_{dc} % values of the PVA/PVP/CMC-TiO_2 NPs nanocomposite samples. The change in the crystalline structure could be referred to as the impact of TiO_2 NPs on the composition of the PVA/PVP/CMC blend matrix. Where this result suggests that adding TiO_2 NPs with strong crystalline properties to the PVA/PVP/CMC ternary polymer blend could physically increase the amorphous areas in the polymer blend, decreasing its semicrystalline nature. This decrease in semi-crystalline nature

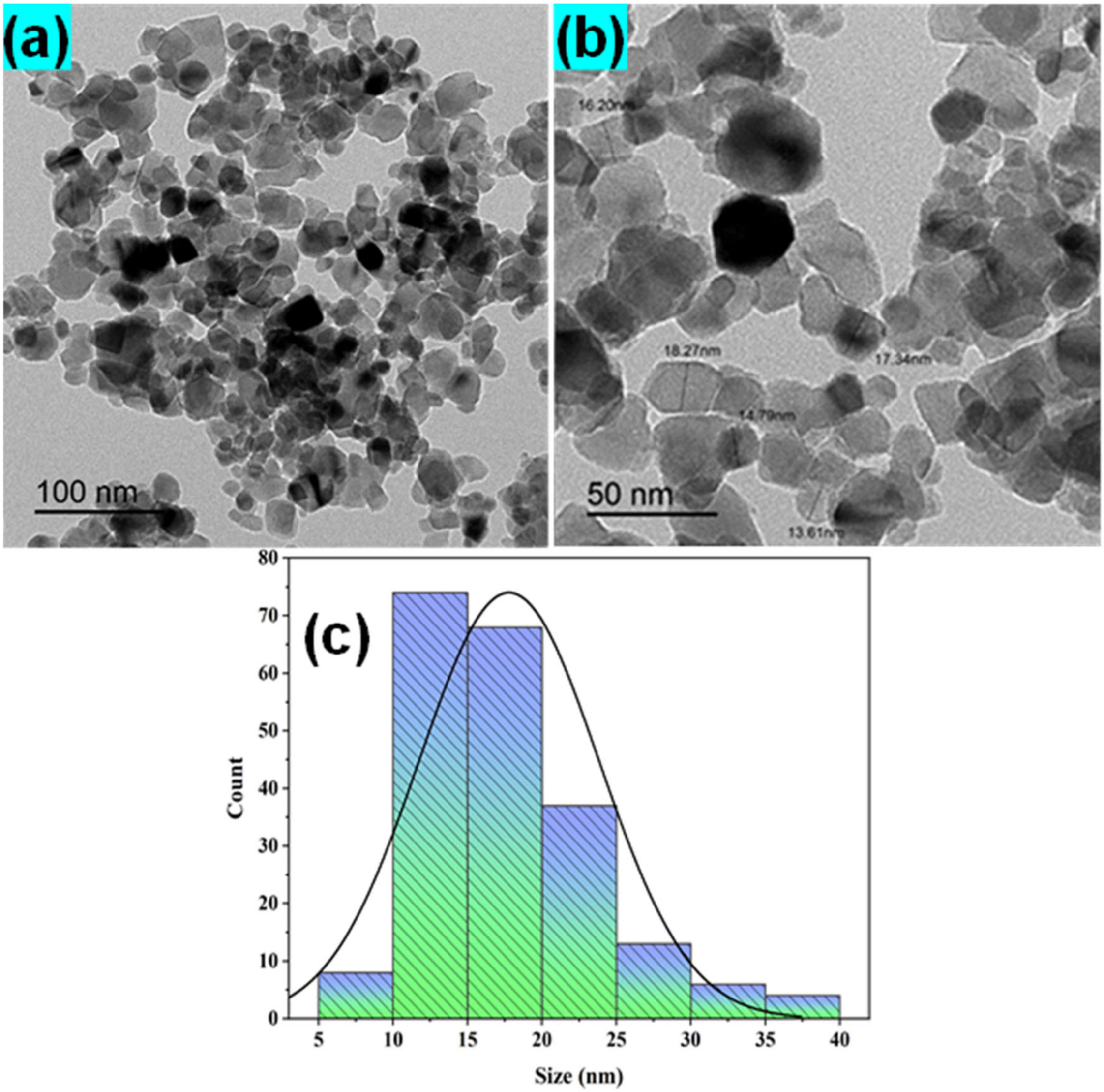

Fig. 3 **a**, **b** The TEM micrographs of the TiO_2 NPs, (**c**) its congruous histograms related to the nanoparticles size distribution

could chemically indicate an increase in disorder caused by a reduction in the number of intermolecular bonds in polymer blend chains. The reduction in the crystalline structure could lead to an increase in ionic mobility and hence electrical conductivity and enhancement in its applicability in energy storage devices.

3.2 TEM analysis

Figure 3a, b shows the TEM micrograph of the TiO_2 NPs prepared by the sol-gel method, besides their congruous histograms, respectively; the histograms reveal the size and distribution sizes. The TEM micrographs show that the TiO_2 NPs have a uniform distribution behavior. Further, the TiO_2 NPs shapes vary from spherical to hexagonal and rectangular. The particle sizes were in the range between 5 and 40 nm; the particle size of the prepared TiO_2 NPs was nearly 17.5 nm.

3.3 FTIR spectroscopy

To estimate the chemical functional groups and changes in the molecular struc-tures, FTIR spectroscopic analysis was conducted for the PVA/PVP/CMC ternary blend and the PNCs filled with TiO_2 NPs contents of 0.5, 1.5, and 3 wt%. In the FTIR spectral charts (Fig. 4), certain bands were observed, including the stretching vibration mode for the -OH group of CMC that centers at 3438 cm^{-1}, and the band at 2940 cm^{-1} could belong to the asymmetrical stretching vibrational mode of the H-C-H. The band centered at 1450 cm^{-1} is assigned to the -CH_2 scissoring vibrational modes [37]. The -CN stretching band of PVP located at

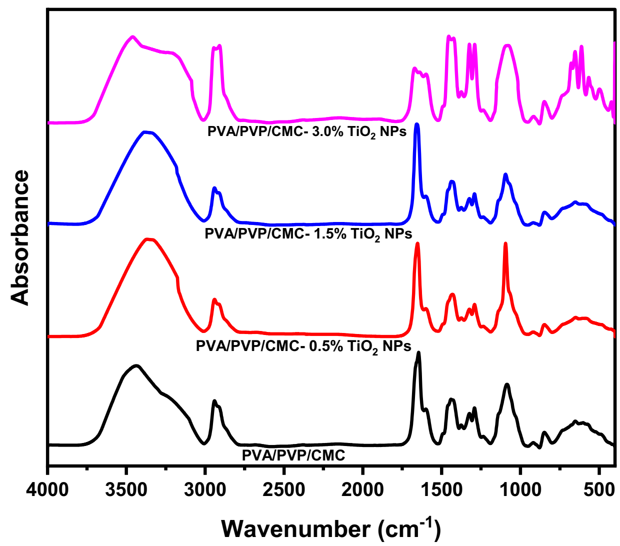

Fig. 4 FTIR spectral charts of the PVA/PVP/CMC ternary blend and the PNCs filled with TiO_2 NPs contents of 0.5, 1.5, and 3 wt%

Table 2 FTIR spectra bands' assignments for the pure blend of ternary polymers of PVA/PVP/CMC and the prepared PNC samples

Wavenumber (cm^{-1})	Band assignment
3438	-OH str.
2940	H-C-H asymmetrical str.
1650	C=O str.
1450	$-CH_2$ scissoring or C=N of pyridine ring
847	–CH rocking
1292	-CN str.
923	-CH bending (out-of-plane rings)
2906	CH_2 symmetrical str. (shoulder)
1030	C-O str. (shoulder)
1600	$-COO^-$ str.
1374	CH_2 bending
1324	-CH or -OH bending
1230	-CH wagging
1086	-OH bending
734	$-CH_2$ rocking
615	-CH wagging

1292 cm^{-1} is attributed to the pyridine ring, while the band observed at 923 cm^{-1} could result from the bending vibration mode of the -CH group [37]. A summary of the assigned bands for the FTIR spectra of the samples can be found in Table 2.

The FTIR spectra of the PNC films prepared exhibited minor shifts in some peaks by comparing with the FTIR spectrum of the blend of ternary polymers alone. For instance, the 3438 cm^{-1} band shifted towards a lower wavenumber to 3357 cm^{-1} after introducing TiO_2 NPs. The intensity of several bands also displayed considerable

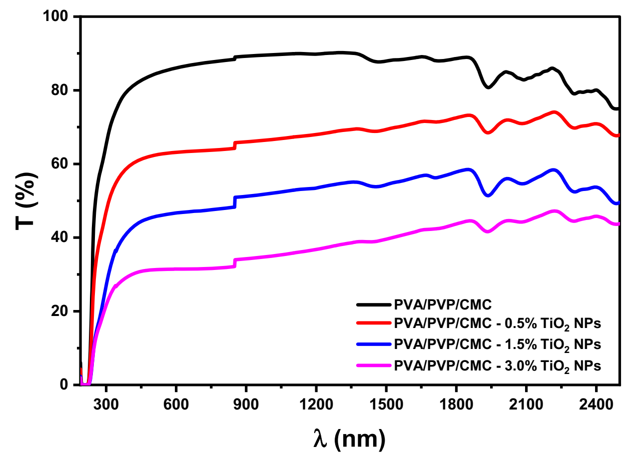

Fig. 5 The UV/VIS spectra in the wavelength region from 190 to 2500 nm for the PVA/PVP/CMC ternary blend and the PNCs filled with TiO_2 NPs contents of 0.5, 1.5, and 3 wt%

variations, which may be attributed to the physicochemical interactions between the ternary polymers' blend matrix and the TiO_2 NPs [38]. The variations in intensity peaks of the PNCs prepared with 0.5%, 1.5%, and 3% TiO_2 content could be attributed to TiO_2 nanofillers. These nanofillers cause an increase in the amorphous phase, as revealed by XRD analysis. The amorphous phase causes decreases in the intermolecular interactions between the chains of the PVA/PVP/CMC ternary blend, resulting in significant changes in the chemical functional groups that appear in the FTIR spectra peaks. Additionally, the two observed FTIR bands noted at nearly 1600 and 1324 cm^{-1} were identified as the asymmetric stretching vibration mode of the carboxylate (−COO−) group and the bending vibration of the hydroxyl group (–OH), respectively. These two functional groups significantly contribute to the likelihood of intermolecular hydrogen bonding between TiO_2 NPs and the PVA/PVP/CMC blend [39], thus improving the structural features of their PNCs. Similar behavior was found in the CMC/polyacrylamide (PAM)/Co_3O_4 [40] and PVA/PVP/CMC/ZnO [31] PNCs films.

Due to the presence of oxygen in the ether linkage, the PVP and CMC polymers could be able to engage in intermolecular hydrogen interactions with various molecules. This results in the formation of a high-intensity band at 1086 cm^{-1}, which is indicative of -OH bending [41]. The enhancements in the intensity of this band could be a sign of the interaction between the polymers that make up the blend.

3.4 Optical properties

UV/VIS–NIR spectroscopy was utilized to understand how the PVA/PVP/CMC blend interacts with TiO_2 NPs and affects the optical behavior of the films. At room temperature, Fig. 5 showcases the PNC films' UV/VIS-NIR

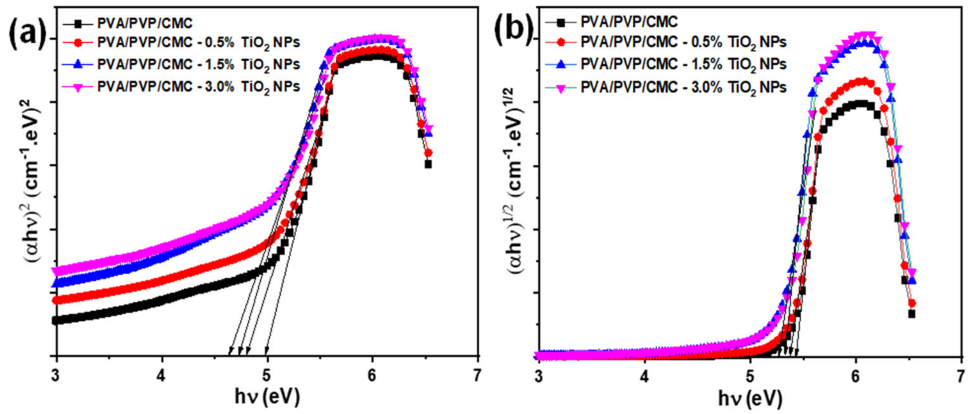

Fig. 6 Plot of (**a**) $(\alpha h\nu)^2$ and (**b**) $(\alpha h\nu)^{1/2}$ as functions of energy ($h\nu$) for the PVA/PVP/CMC ternary blend and the PNCs filled with TiO_2 NPs contents of 0.5, 1.5, and 3 wt%

transmittance spectra, prepared based on PVA/PVP/CMC and TiO_2 in the 190–2500 nm wavelength range. The UV spectrum exhibited a sharp edge at around 242 nm, with a noticeable difference in height between the pure blend and PNC samples. This variation might be attributed to the disorder caused by the presence of TiO_2 NPs in the polymers' host matrices. It's possible that the change observed is a result of the presence of amorphous areas within the PVA/PVP/CMC matrix alongside some crystalline regions. These findings confirm the XRD results, indicating that the prepared PNC samples are semicrystalline in nature. Additionally, the shift in the edge position from 242 nm to 255 nm clearly could suggest successful complexation between the constituents of the nanocomposites. The charge transfer absorption bands result primarily from electronic transitions, where the transitions occur from the highest occupied molecular orbital to the lowest unoccupied molecular orbital. As such, the band located around ≈ 204 nm is identified as the $n \rightarrow \pi^*$ transition [42].

The optical direct (E_{gd}) and indirect (E_{gi}) energy gap of the pure polymers' blend and PNC samples were determined using Tauc's plots, as shown in Fig. 6a, b, respectively. From these plots, the E_{gd} and E_{gi} energy gaps were calculated. A summary of the calculated direct and indirect optical band gaps can be found in Table 1. According to the collected data, the inclusion of TiO_2 NPs caused a considerable reduction in the E_g values. Among all the nanocomposites, the PVA/PVP/CMC-1.5% TiO_2 PNC demonstrated the lowest E_g value, making it the most favorable option. These reductions in E_g values could be referred to as the presence of various polaronic contributions and imperfections that often occur in PVA/PVP/CMC-based PNCs. It has been observed that the movement direction of charge carriers is from a lower to a higher energy level during indirect transfer, as this requires only a minimal energy amount to have occurred [40]. On the other hand, direct transition necessitates a considerably larger energy amount. In contrast, the direct transition requires more energy amount. This illustration could illustrate why E_{gd}'s values are greater than E_{gi}'s.

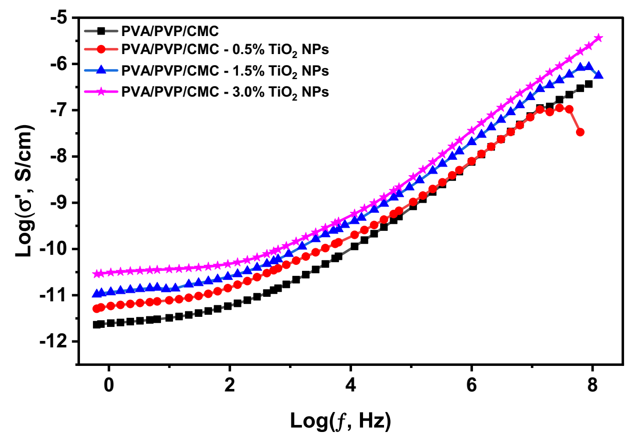

Fig. 7 The variation of conductivity (Log σ) versus frequency (Log f) at RT for the PVA/PVP/CMC ternary blend and the PNCs filled with TiO_2 NPs contents of 0.5, 1.5, and 3 wt%

The refractive index (n) values were obtained by inputting the E_g values into Eq. (3) provided in reference [43]. The findings have been compiled and presented in Table 1

$$\frac{n^2 - 1}{n^2 + 2} = 1 - \sqrt{\frac{E_g}{20}} \quad (3)$$

The increase in the prepared PNC films' refractive index by comparing it with that of the pure polymers' blend could be understood through the increase in the optical density of the PNC films. The optical density could increase because of the TiO_2 NPs incorporation into the polymeric matrix, which finally impacted the light penetration velocity.

3.5 Electric analysis

Figure 7 depicts the alternative current electrical conductivity (Log σ_{ac}) variation versus frequency (Log f) at room temperature for the virgin PVA/PVP/CMC ternary blend and the PNC films with nanofiller, i.e., TiO_2 NPs. It can be seen that the σ values of the prepared samples are enhanced with the loading of the TiO_2 nanofiller. The observed dispersions in the low-frequency domain are owing

Table 3 The calculated value of DC conductivity (σ_{dc}), exponentiation factor (s), and ε' (100 Hz) for the present films

Sample	σ_{dc}(S cm^{-1})	s	$\varepsilon'_{\text{at 100 Hz}}$
Pure PVA/PVP/CMC	2.30×10^{-12}	0.93	2.5
PVA/PVP/CMC −0.5%Ti NPs	5.90×10^{-12}	0.82	4
PVA/PVP/CMC −1.5%Ti NPs	1.11×10^{-11}	0.86	6.5
PVA/PVP/CMC −3.0%Ti NPs	2.88×10^{-11}	0.89	10

to electrode polarization or spatial charge. The TiO_2 nanofiller could help to decrease potential barriers and works towards connecting two localized states, which facilitates the movement of charge carriers [44]. The relatively high conductivity of the TiO_2 NPs (~22×10^{-7} S cm^{-1}) [45] also contributes to these improvements in σ_{ac} values of the produced PNCs. The enhanced amorphous area in PNCs samples may be responsible for this improvement in the movement of charge carriers. Jonscher's power law can represent electrical conductivity based on the following equation:

$$\sigma(\omega) = \text{DC electrical conductivity} + \text{A}(\text{angular frequency})^s = \sigma_{dc} + \text{A}\omega^s \tag{4}$$

where, s denotes the exponentiation factor. The obtained values of σ_{dc} and s are summarized in Table 3. The behavior of σ_{ac} (Fig. 7) indicates that the conduction mechanism of charge carriers in these materials utilized a correlated barrier hopping mechanism proposed by Pike [46] and Elliot [47]. It can be seen that the obtained values of σ_{dc} for the prepared PNCs samples reached 2.88×10^{-11} S cm^{-1} for the last sample. It is known that the number of charge carriers and their mobility determine the polymeric material's conductivity. These factors can be changed by varying the amount of nanofiller present in the host ternary polymer matrix. It suggests that the adding of TiO_2 NPs in the PVA/PVP/CMC ternary blend increased the favorable sites and/or presented some additional charge carriers; as a result, there may have been an improvement in the mobility and density of charge carriers, leading to an increase in σ values for the prepared PNCs samples. The increase in the values of both σ_{dc} and σ_{ac} indicates that these PNCs may be considered suitable applicants for electronic devices, for instance, flexible polymeric dielectric capacitors [48, 49]. Although the content of TiO_2 affects the conductivity of the prepared PNC systems, it must mention here no abrupt increase in the conductivity while applying this study.

3.6 Dielectric properties

The dielectric constant, ε', describes the energy that has been stored in a sample, whereas the dielectric loss, ε'', describes the energy that the sample dissipates in reaction to an outside electric field.

The values of ε' and ε'' of the samples under examination beside the dielectric loss tangent (tan δ) were determined using the following equations in terms of the capacitance (C) and the free space permittivity (ε_o) [50–52]:

$$\varepsilon' = \frac{\text{Cd}}{\varepsilon_o A} \tag{5}$$

$$\varepsilon'' = \frac{\sigma}{\omega\varepsilon_o} \tag{6}$$

$$\tan\delta = \frac{\varepsilon'}{\varepsilon''} \tag{7}$$

Figure 8a, b illustrates how ε' and ε'' values vary for all prepared PNCs films in response to various frequencies at room temperature. The obtained ε' and ε'' spectra are observed to decrease nonlinearly when the frequencies increase. They improved when adding the TiO_2 nanofillers, and similar behavior was reported in various polymers [53, 54]. At lower frequencies, interfacial polarization causes increased values of ε' for the produced PNCs samples, but at higher frequencies, the value of the dielectric constant is independent of the frequency. But as the frequency of the field increases, this value gradually decreases due to the inability of all types of polarization to follow the changes in the electric field direction [40, 55]. Thus, high frequencies have a reasonably constant complex permittivity with frequency. After the addition of TiO_2 nanofillers, the amount of parallel aligned dipoles in the pure ternary blend matrix increased, as evidenced by an increase in the values ε'; for instance, at 10 Hz, the value of ε' for the prepared PNCs films is high in comparison to that of the pure ternary polymers' blend matrix (see Fig. 8a and Table 3). The difference between the nature of the nanofiller (TiO_2 NPs) and the host polymers' blend led to the formation of micro-capacitors over the whole volume of PNCs samples [56, 57]. Additionally, it can be seen that the behavior of ε″ for all prepared PNC samples exhibits the same pattern of ε' as observed in Fig. 8b. Also, the obtained dielectric constant value at 10 Hz in this work for PVA/PVP/CMC-5% TiO_2 NPs was better than some of those mentioned in the literature (Table 4). Table 4 lists a comparison between the value of σ_{dc} and ε' at 10 Hz obtained by this work and the published works [31, 43, 58–61].

Figure 8c displays tanδ variation versus frequency for prepared PNCs. It can be observed that PNCs with 0.5%, 1.5%, and 3% TiO_2 exhibit similar behavior compared to pure blend PVA/PVP/CMC. The results in Fig. 8a, c suggest that although the tanδ is not as small as reported in the published works [62–64], it is still enhanced compared to a pure ternary polymer blend. These results could indicate that the addition of TiO_2 NPs enhances the blend's energy

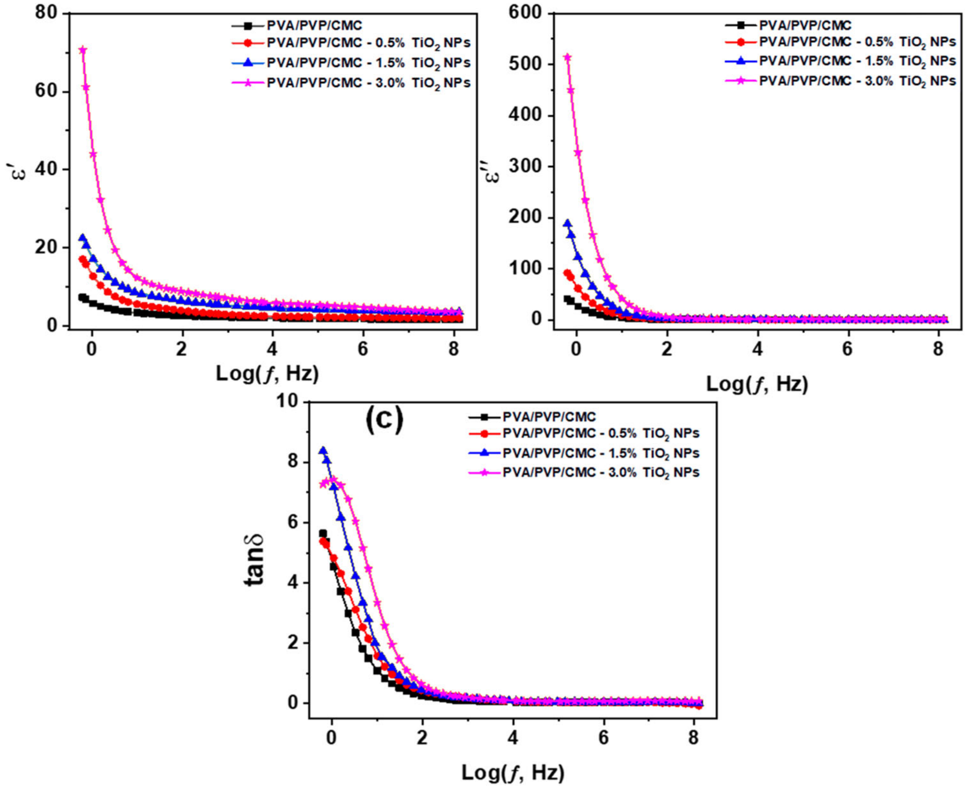

Fig. 8 The variation of dielectric properties versus frequency for the PVA/PVP/CMC ternary blend and the PNCs filled with TiO_2 NPs contents of 0.5, 1.5, and 3 wt.% (**a**), ε′ (**b**) ε″, and (**c**) tan δ

Table 4 The σ_{dc} and ε' at 10 Hz recorded by this study and literature [31, 43, 58–61]

Work	Polymers	Filler	σ_{dc}(S cm^{-1})	ε'
[31]	PVA/PVP/CMC	ZnO NPs (5% wt.)	~3.16×10^{-11}	~17
[43]	PVA/CMC	$SrTiO_3$ (6%wt.)	~1.84×10^{-10}	~15
[58]	CMC/PVA/ graphene nanoplatelets	ZnO NPs (6%)	~1.38×10^{-10}	~12.8
[59]	PVA/PEO	ZnO NPs (5%)	~15.9×10^{-12}	~5.5
[60]	PVP/PEO	MoO_3 NPs (6%wt.)	~5.60×10^{-9}	~20
[61]	Polystyrene /polyvinyl carbazole	TiO_2 NPs (5%wt.)	~4.07×10^{-13}	~2.5
This work	(PVA/PVP/CMC)	TiO_2 NPs (3%wt.)	~2.88×10^{-11}	~9.25

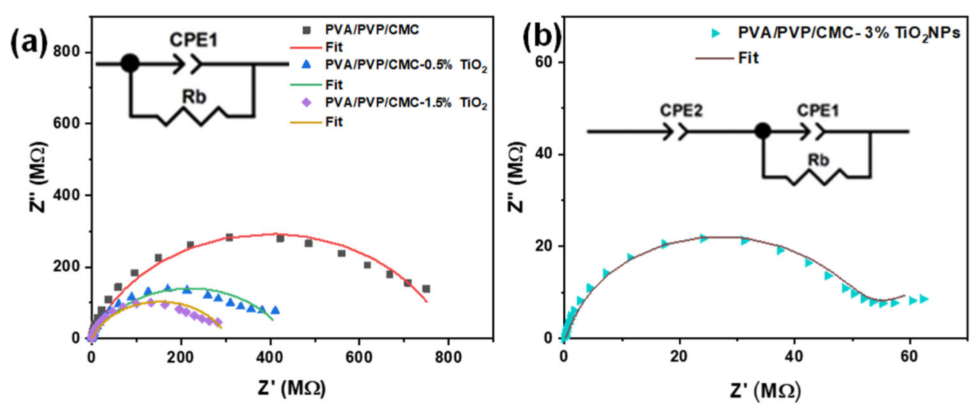

Fig. 9 The Nyquist plot (Z' versus Z'') of the PVA/PVP/CMC ternary blend and the PNCs filled with TiO_2 NPs contents of 0.5, 1.5, and 3 wt% (asterisks are the experimental data, and the solid line denotes the fitting findings)

storage ability without increasing energy dissipation. Therefore, PNCs of this ternary polymer blend with TiO_2 are promising nanocomposites for energy storage applications.

3.7 Impedance analysis

Figure 9a, b depicts the Nyquist plot (Z' versus Z'') of the prepared PVA/PVP/CMC-TiO_2 samples. The conductive properties of the bulk material are represented by semicircles in the higher frequencies, while the tail is created at low frequencies as a result of the influence of the electrical double layer [65]. The semicircles' radii get smaller and smaller as they go closer to their origin. This suggests that the addition of TiO_2 nanofiller to the polymers' blend matrix could cause an increase in the disorder areas, which is supported by XRD, leading to increases in the ionic conductivity of the PNC films.

Using EIS software, the resulting Z'' versus Z' data were fitted and found equal to a circuit combination. The components of this circuit are the bulk resistance (Rb) and the constant phase element (CPE) (there are two elements found in the equivalent circuit, CPE1 and CPE2). The impedances of the CPE1 and CPE2 are calculated using the following formula [66]:

$$\mathrm{ZCPE} = 1/Q(iw)^n \tag{8}$$

The symbol Q represents the numerical value of $1/Z$ at = 1 rad/s, while n refers to the phase of the element and indicates the deviation degree from a pure capacitor. Table 5 lists the determined fitting elements. It is worth mentioning that when the TiO_2 NPs were added to the prepared ternary blend, the value of (Rb) for the filled PNCs decreased compared to the value for the pure mixture, indicating that the charge transfer became more accessible inside the PNCs.

Table 5 The obtained parameters for fitting equivalent circuit models

Sample	Rb (Ω)	Q_1 (F)	n_1	Q_2 (F)	n_2
PVA/PVP/CMC	7.98×10^8	2.73×10^{-10}	0.80		
PVA/PVP/CMC-0.5%TiO_2	4.38×10^8	4.79×10^{-10}	0.72		
PVA/PVP/CMC-1.5%TiO_2	3.06×10^8	5.42×10^{-10}	0.76		
PVA/PVP/CMC-3.0%TiO_2	4.79×10^7	7.49×10^{-10}	0.90	8.62×10^{-8}	0.35

3.8 Dielectric Modulus

The electric modulus is the physical principle that is used to investigate the electrical relaxation mechanism of materials with ionic conductivities. Physically, electric moduli, i.e., M' and M'' are used to study the electric field relaxation in the materials when the electric displacements stay constant [67]. The prepared PNC films M' and M'' measured at room temperature are illustrated in Fig. 10a, b. The dependency of M' on the frequency spectrum is depicted in Fig. 10a. The M′ modulus is known as the retrograde quantity of the dielectric constant; as observed in Fig. 8a, the dielectric constant recorded higher values at lower frequencies and lower values at higher frequencies. Therefore, the M'

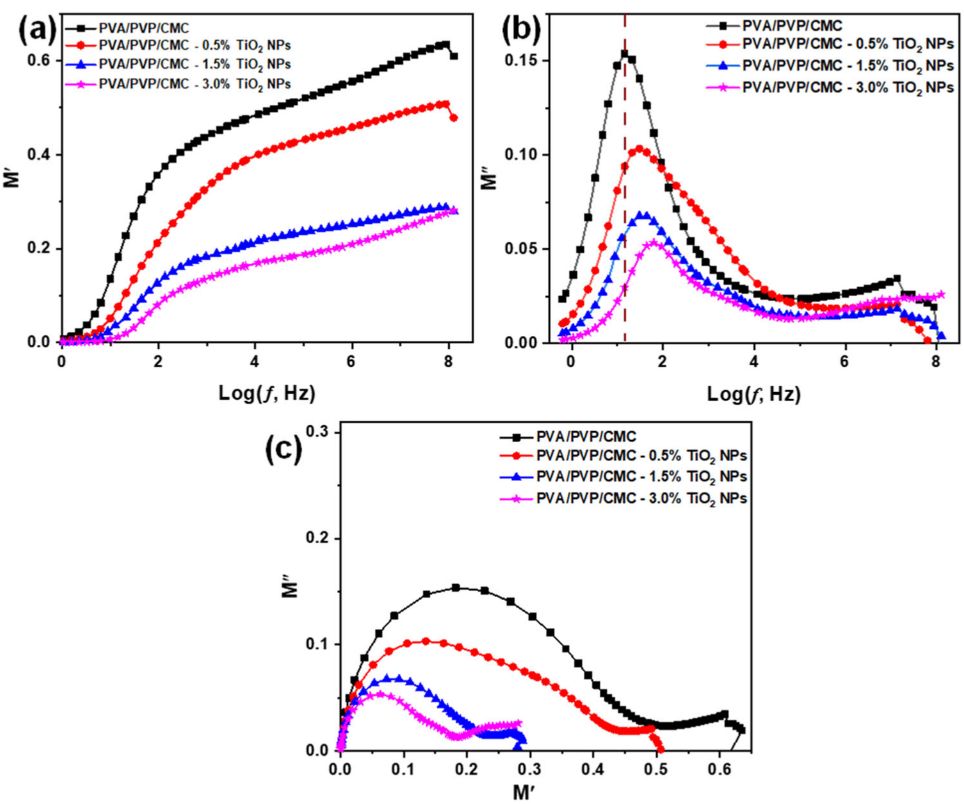

Fig. 10 The variation of (**a**) M' and (**b**) M'' versus frequency; (**c**) the plot of M–M'' behavior for the PVA/PVP/CMC ternary blend and the PNCs filled with TiO_2 NPs contents of 0.5, 1.5, and 3 wt%

modulus values are as expected; the M' modulus recorded the reverse behavior for the dielectric constant. It was observed that, at low frequencies, M' seems to be zero for either the pure blend polymer or PNCs with nanofiller contents (Fig. 10a). This result suggests that the contribution of the electrode/electrolyte polarization could be considered negligible [68]. Also, all PNCs reach the saturation stage at high frequencies, with M' values increasing steadily with increasing frequency (Fig. 10a). This increase in M' value is due to the electrical conductivity related to the charge/ion carriers' short-range mobility. Also, this conduct was reported [69, 70] in several PNCs systems. It can also observe that the M' values decreased while increasing the TiO_2 nanofillers in the polymer matrix compared to the M' values of the pure ternary polymers; this result could suggest the effect of TiO_2 NPs in the ionic conductivity of the polymer matrix. This attitude affirms that the relaxation depends upon TiO_2 nanofiller.

The spectrum imaginary electric modulus, M'', of the pure ternary polymers' blend and the PNCs filled with TiO_2 NPs contents of 0.5, 1.5, and 3 wt% reveals a relaxation peak (Fig. 10b). It can be noticed M'' modulus manifests for the pure polymer blends, and PNCs samples a single relaxation peak that could be attributed to dc-conductivity contribution. As shown in Fig. 10b, the M'' modulus relaxation peak shifted to a higher frequency when introducing the TiO_2 nanofillers and continued shifting with increasing the nanofiller content. Also, it can be observed clearly, that the maximum peak of in the M'' modulus decreased considerably with the increase in the TiO_2 nanofillers content. As TiO_2 nanofiller content increased to 3 weight percent, its intensity diminished, and its location changed. This finding suggests the possible effect of TiO_2 nanofillers on the dc-conductivity contribution. Also, in the relaxation peak in the M'' modulus curves, there are two parts. The first part is on the left side of the relaxation peak (at low frequency); this part represents the region of frequency in which the ions move over long distances, where the ions can easily jump between the neighbor sites. The second part is on the right side of the relaxation peak (at high frequency), where ions are trapped in their potential wells and can perform only localized motion. Asymmetry peak broadening can be noticed in the relaxation peaks, suggesting different time constants where it was found that the dielectric relaxation time (τ) [$\tau \approx 1/\omega$] decreased considerably from 69 to 16 ms. This result could point out the non-Debye type of relaxation in the prepared PNC samples.

4 Conclusion

TiO_2 NPs were prepared via sol-gel technique; then, they were used as nanofillers with the ternary polymers' blend of PVA/PVP/CMC to prepare PNC films. The structures, morphologies, and optical properties of the prepared pure blend polymers and the PNC films with TiO_2 NPs contents of 0.5, 1.5, and 3 wt% were thoroughly examined using XRD, FTIR, TEM, and UV/VIS–NIR techniques. These techniques revealed comparatively good interactions between polymer chains and the nanofiller. The structural investigation showed that the prepared PNC samples have semicrystalline nature owing to the structure of the PVA polymer, and the addition of TiO_2 NPs significantly reduced the crystallinity ratio. At the same time, the optical measurements for the ternary PNC film filled with 3% wt TiO_2 exhibit decreasing in the E_g value with increasing the content of the TiO_2 nanofillers. Applying these prepared PNC films, the electrical and dielectric properties were investigated to assess their suitability for dielectric capacitors. The electrical and dielectric results revealed that the ε', ε, M', M'', and σ_{ac} values were enhanced after loading the TiO_2 NPs. Also, the DC conductivity increased from $2.30 \times 10^{-12}\,S\,cm^{-1}$ (for pure PVA/PVP/CMC blend) to $2.88 \times 10^{-11}\,S\,cm^{-1}$ (for 3% TiO_2 NPs). From the impedance spectra, it was found that the semicircles' radii in the Nyquist plot (Z' versus Z'') of the prepared PNCs with TiO_2 NPs samples became smaller as the TiO_2 NPs content increased. The M' results indicate that the contribution of electrode/electrolyte polarization might be considered negligible. Furthermore, M' and M'' values decreased as the TiO_2 nanofillers content increased in the polymer matrix. The outcomes and improved electrical and dielectric features of the PNC films suggest that these samples could be suitable for flexible energy storage applications, such as capacitors and batteries.

Data availability

The data that support the findings of this study are available from the corresponding author upon reasonable request.

Acknowledgements This research work was funded by Institutional Fund Project under grant no. (IFPIP: 1871-135-1443). The authors gratefully acknowledge technical and financial support provided by the Ministry of Education and King Abdulaziz University, DSR, Jeddah, Saudi Arabia.

Author contributions MMD: Project Administration, Methodology, Review & Editing, Formal Analysis, Validation, Visualization, Funding Acquisition. AS: Supervision, Conceptualization, Methodology, Resources, Software, Data Curation, Writing—Original Draft, Review & Editing, Formal Analysis, Validation, Visualization. EMA: Writing - Original Draft, Review & Editing Formal Analysis. AMA: Writing—Original Draft, Review & Editing Formal Analysis. AYY: Conceptualization, Software, Review & Editing, Formal Analysis, Validation, Visualization. JAMA: Writing, Review & Editing. AAA-M: Supervision, Conceptualization, Methodology, Resources, Software, Data Curation, Writing—Original Draft, Review & Editing, Formal Analysis, Validation, Visualization. All authors reviewed the manuscript.

Compliance with ethical standards

Conflict of interest The authors declare no competing interests.

References

1. Selvi J, Parthasarathy V, Mahalakshmi S, Anbarasan R, Daramola MO, Senthil Kumar P (2020) Optical, electrical, mechanical, and thermal properties and non-isothermal decomposition behavior of poly (vinyl alcohol)–ZnO nanocomposites. Iran Polym J 29(5):411–422
2. Wonci Z, Tsolekile N, Matoetoe M (2022) Polyvinylpyrrolidone as a polymer template for CuInS quantum dots: effect on optical properties. Mater Today: Proc 56:1989–1994
3. AlSaidi RA, Alamri HR, Sharma K, Al-Muntaser A (2022) Insight into electronic structure and optical properties of ZnTPP thin films for energy conversion applications: experimental and computational study. Mater Today Commun 32:103874
4. Yu J, Yang J, Liu B, Ma X (2009) Preparation and characterization of glycerol plasticized-pea starch/ZnO–carboxymethylcellulose sodium nanocomposites. Bioresour Technol 100(11):2832–2841
5. Ghanbarzadeh B, Almasi H, Oleyaei SA (2013) A novel modified starch/carboxymethyl cellulose/montmorillonite bionanocomposite film: structural and physical properties. Int J Food Eng 10(1):121–130
6. Al-Muntaser AA, Pashameah RA, re A, Alwafi R, Alzahrani E, AlSubhi SA, Yassin AY (2023) Boosting the optical, structural, electrical, and dielectric properties of polystyrene using a hybrid GNP/Cu nanofiller: novel nanocomposites for energy storage applications. J Mater Sci-Mater Electron 34(7):678. https://doi.org/10.1007/s10854-023-10104-7
7. Saeed A, Abolaban F, Al-Mhyawi SR, Albaidani K, Al Garni SE, Al-Marhaby FA, Alwafi R, Djouider F, Qahtan TF, Asnag GM (2023) Improving the polyethylene oxide/carboxymethyl cellulose blend's optical and electrical/dielectric performance by incorporating gold quantum dots and copper nanoparticles: nanocomposites for energy storage applications. J Mater Res Technol-JMRT 24:8241–8251. https://doi.org/10.1016/j.jmrt.2023.05.073
8. El Gohary HG, Alhagri IA, Qahtan TF, Al-Hakimi AN, Saeed A, Abolaban F, Alshammari EM, Asnag GM (2023) Reinforcement of structural, thermal and electrical properties and antibacterial activity of PVA/SA blend filled with hybrid nanoparticles (Ag and TiO2 NPs): nanodielectric for energy storage and food packaging industries. Ceram Int 49(12):20174–20184. https://doi.org/10.1016/j.ceramint.2023.03.141
9. Al-Muntaser AA, Pashameah RA, Tarabiah AE, Alzahrani E, AlSubhi SA, Saeed A, Al-Harthi AM, Alwafi R, Morsi MA (2023) Structural, morphological, optical, electrical and dielectric features based on nanoceramic $Li_4Ti_5O_{12}$ filler reinforced PEO/PVP blend for optoelectronic and energy storage devices. Ceram Int 49(11, Part B):18322–18333. https://doi.org/10.1016/j.ceramint.2023.02.204
10. Gabal MA, Al-Harthy EA, Al Angari YM, Awad A, Al-Juaid AA, Saeed A (2023) Synthesis, characterization and electrical properties of polypyrrole/Mn0.8Zn0.2Fe2O4/GO ternary hybrid composites using spent Zn-C batteries. J Sol-Gel Sci Technol https://doi.org/10.1007/s10971-023-06053-6
11. Rajabathar JR, Arunachalam P, Al-Lohedan HA, Thankappan R, Appaturi JN, Pulingam T, Mohammed Dahan W (2021) Polymer surfactant (Triton-100) assisted low cost method for preparing silver and graphene oxide modified Bi-MnOx nanocomposite for enhanced sensor and anti-microbial health care applications. J Sol-Gel Sci Technol 97(3):638–650. https://doi.org/10.1007/s10971-021-05468-3
12. Erdem B, İşcan KB (2021) Multifunctional magnetic mesoporous nanocomposites towards multiple applications in dye and oil adsorption. J Sol-Gel Sci Technol 98(3):528–540. https://doi.org/10.1007/s10971-021-05528-8
13. Ahmed HT, Abdullah OG (2019) Preparation and composition optimization of PEO:MC polymer blend films to enhance electrical conductivity. Polymers 11(5):853. https://doi.org/10.3390/polym11050853
14. Abdullah OGH, Hanna RR, Salman YAK (2019) Structural and electrical conductivity of CH:MC bio-poly-blend films: optimize the perfect composition of the blend system. Bull Mater Sci 42(2):64. https://doi.org/10.1007/s12034-019-1742-3
15. Aziz SB, Ahmed MJ, Abdullah OG, Murad AR, Hamad SM, Hadi JM (2023) Magnesium ion conducting biopolymer blend-based electrolyte for energy storage application: electrochemical characteristics. Electrochim Acta 461:142659. https://doi.org/10.1016/j.electacta.2023.142659
16. Ghanbarzadeh B, Almasi H (2011) Physical properties of edible emulsified films based on carboxymethyl cellulose and oleic acid. Int J Biol Macromol 48(1):44–49
17. Omar A, Ali MS, Abd Rahim N (2020) Electron transport properties analysis of titanium dioxide dye-sensitized solar cells (TiO2-DSSCs) based natural dyes using electrochemical impedance spectroscopy concept: a review. Sol Energy 207:1088–1121. https://doi.org/10.1016/j.solener.2020.07.028
18. Jian Z, Yang N, Vogel M, Zhou Z, Zhao G, Kienitz P, Schulte A, Schönherr H, Jiao T, Zhang W, Jiang X (2020) Tunable photoelectrochemistry of patterned TiO2/BDD heterojunctions. Small Methods 4(9):2000257. https://doi.org/10.1002/smtd.202000257
19. Li R, Ma X, Li J, Cao J, Gao H, Li T, Zhang X, Wang L, Zhang Q, Wang G, Hou C, Li Y, Palacios T, Lin Y, Wang H, Ling X (2021) Flexible and high-performance electrochromic devices enabled by self-assembled 2D TiO2/MXene heterostructures. Nat Commun 12(1):1587. https://doi.org/10.1038/s41467-021-21852-7
20. Sertel BC, Sonmez NA, Kaya MD, Ozcelik S (2019) Development of MgO:TiO_2 thin films for gas sensor applications. Ceram Int 45(3):2917–2921. https://doi.org/10.1016/j.ceramint.2018.11.079
21. Sebak MA, Qahtan TF, Asnag GM, Abdallah EM (2022) The role of TiO_2 nanoparticles in the structural, thermal and electrical properties and antibacterial activity of PEO/PVP blend for energy storage and antimicrobial application. J Inorg Organomet Polym Mater 32(12):4715–4728. https://doi.org/10.1007/s10904-022-02440-8
22. Yu H-F, Cheng C-W (2021) Enhancing photocatalytic ability of TiO_2 films using gel-derived P/Si-TiO2 powder. J Sol-Gel Sci Technol 97(2):259–270. https://doi.org/10.1007/s10971-020-05450-5
23. Chen L, Tao Y, Shang H, Ma Z, Li S, Cao H, Li Q, Li G, Li H, Xiao S, Zhang D (2022) Rutile TiO_2 nanorods grown on carbon nanotubes as high-performance lithium-ion batteries anode via one-dimensional electron pathways. J Sol-Gel Sci Technol 103(2):437–446. https://doi.org/10.1007/s10971-022-05835-8
24. Khoroshko L, Borisenko V, Baltrukovich P, Nurmonov S, Ruzimuradov O (2022) One-step sol-gel fabrication of TiO_2/(CuO +Cu_2O) photocatalysts. J Sol-Gel Sci Technol https://doi.org/10.1007/s10971-022-05906-w
25. Boudiar M, Hanini F, Bouabellou A, Bouachiba Y, Taabouche A, Dergham D, Redjeb C (2023) Sol–gel derived Zn doped TiO2 thin films and their waveguides. J Sol-Gel Sci Technol 107(2):430–440. https://doi.org/10.1007/s10971-023-06133-7
26. Almashhori K, Ali TT, Saeed A, Alwafi R, Aly M, Al-Hazmi FE (2020) Antibacterial and photocatalytic activities of controllable (anatase/rutile) mixed phase TiO_2 nanophotocatalysts synthesized via a microwave-assisted sol–gel method. N J Chem 44(2):562–570. https://doi.org/10.1039/C9NJ03258D

27. Abdel-Galil A, Ali H, Atta A, Balboul M (2014) Influence of nanostructured TiO2 additives on some physical characteristics of carboxymethyl cellulose (CMC). J Radiat Res Appl Sci 7(1):36–43
28. Ezati P, Riahi Z, Rhim J-W (2022) CMC-based functional film incorporated with copper-doped TiO2 to prevent banana browning. Food Hydrocoll 122:107104
29. Ren J, Wang S, Gao C, Chen X, Li W, Peng F (2015) TiO_2-containing PVA/xylan composite films with enhanced mechanical properties, high hydrophobicity and UV shielding performance. Cellulose 22(1):593–602
30. Bisen R, Tripathi J, Sharma A, Khare A, Kumar Y, Tripathi S (2018) Optical behaviour of coumarin dye in PVA and PMMA film matrices. Vacuum 152:65–69
31. Al-Muntaser AA, Alzahrani E, Abo-Dief HM, Saeed A, Alshammari EM, Al-Harthi AM, Tarabiah AE (2023) Tuning the structural, optical, electrical, and dielectric properties of PVA/PVP/CMC ternary polymer blend using ZnO nanoparticles for nanodielectric and optoelectronic devices. Opt Mater 140:113901. https://doi.org/10.1016/j.optmat.2023.113901
32. Morsi MA, Pashameah RA, Sharma K, Alzahrani E, Farea MO, Al-Muntaser AA (2022) Hybrid MWCNTs/Ag nanofiller reinforced PVP/CMC blend-based polymer nanocomposites for multifunctional optoelectronic and nanodielectric applications. J Polym Environ https://doi.org/10.1007/s10924-022-02656-2
33. Chen Y-N, Jiao C, Zhao Y, Zhang J, Wang H (2018) Self-assembled polyvinyl alcohol–tannic acid hydrogels with diverse microstructures and good mechanical properties. ACS Omega 3(9):11788–11795. https://doi.org/10.1021/acsomega.8b02041
34. Aziz SB, Abdulwahid RT, Rasheed MA, Abdullah OG, Ahmed HM (2017) polymer blending as a novel approach for tuning the spr peaks of silver nanoparticles. Polymers 9(10) https://doi.org/10.3390/polym9100486
35. Achachlouei BF, Zahedi Y (2018) Fabrication and characterization of CMC-based nanocomposites reinforced with sodium montmorillonite and TiO_2 nanomaterials. Carbohydr Polym 199:415–425. https://doi.org/10.1016/j.carbpol.2018.07.031
36. Hermans PH, Weidinger A (1949) X-ray studies on the crystallinity of cellulose. J Polym Sci 4(2):135–144. https://doi.org/10.1002/pol.1949.120040203
37. Elashmawi I, Abdelrazek E, Yassin A (2014) Influence of $NiCl_2$/$CdCl_2$ as mixed filler on structural, thermal and electrical properties of PVA/PVP blend. Br J Appl Sci Technol 4(30):4263
38. Gunathilake TMSU, Ching YC, Chuah CH, Hai ND, Nai-Shang L (2020) Electro-stimulated release of poorly water-soluble drug from poly (lactic acid)/carboxymethyl cellulose/ZnO nanocomposite film. Pharm Res 37(9):1–20
39. Cuevas JC, Heurich J, Pauly F, Wenzel W, Schön G (2003) Theoretical description of the electrical conduction in atomic and molecular junctions. Nanotechnology 14(8):R29
40. Elashmawi I, Al-Muntaser A (2021) Influence of Co_3O_4 nanoparticles on the optical, and electrical properties of CMC/PAM polymer: combined FTIR/DFT study. J Inorg Organomet Polym Mater 31(6):2682–2690
41. Abdelrazek E, Elashmawi I, El-Khodary A, Yassin A (2010) Structural, optical, thermal and electrical studies on PVA/PVP blends filled with lithium bromide. Curr Appl Phys 10(2):607–613
42. Sengwa RJ, Choudhary S, Dhatarwal P (2019) Nonlinear optical and dielectric properties of TiO_2 nanoparticles incorporated PEO/PVP blend matrix based multifunctional polymer nanocomposites. J Mater Sci-Mater Electron 30(13):12275–12294
43. Al-Muntaser A, Pashameah RA, Sharma K, Alzahrani E, Hameed S, Morsi M (2022) Boosting of structural, optical, and dielectric properties of PVA/CMC polymer blend using SrTiO3 perovskite nanoparticles for advanced optoelectronic applications. Opt Mater 132:112799
44. Atta M, Alsulami QA, Asnag G, Rajeh A (2021) Enhanced optical, morphological, dielectric, and conductivity properties of gold nanoparticles doped with PVA/CMC blend as an application in organoelectronic devices. J Mater Sci-Mater Electron 32(8):10443–10457
45. Othman MA, Amat NF, Ahmad BH, Rajan J (2014) Electrical conductivity characteristic of TiO_2 nanowires from hydrothermal method. J Phys: Conf Ser 1:012027. IOP Publishing, p
46. Pike G (1972) AC conductivity of scandium oxide and a new hopping model for conductivity. Phys Rev B 6(4):1572
47. Elliott S (1987) Ac conduction in amorphous chalcogenide and pnictide semiconductors. Adv Phys 36(2):135–217
48. Xu F, Zhang H, Jin L, Li Y, Li J, Gan G, Wei M, Li M, Liao Y (2018) Controllably degradable transient electronic antennas based on water-soluble PVA/TiO_2 films. J Mater Sci 53(4):2638–2647
49. Deshmukh K, Ahamed MB, Sadasivuni KK, Ponnamma D, AlMaadeed MAA, Deshmukh RR, Pasha SK, Polu AR, Chidambaram K (2017) Fumed SiO_2 nanoparticle reinforced biopolymer blend nanocomposites with high dielectric constant and low dielectric loss for flexible organic electronics. J Appl Polym Sci 134 (5)
50. Saeed A, Madkhli AY, Al-Dossari M, Abolaban F (2022) Electrical and dielectric properties of composites composed of natural quartz with aluminum. Silicon 14(15):9517–9531. https://doi.org/10.1007/s12633-022-01713-8
51. Saeed A, Al-Buriahi MS, Razvi MAN, Salah N, Al-Hazmi FE (2021) Electrical and dielectric properties of meridional and facial Alq_3 nanorods powders. J Mater Sci-Mater Electron 32(2):2075–2087. https://doi.org/10.1007/s10854-020-04974-4
52. Saeed A, Adewuyi SO, Ahmed HAM, Alharbi SR, Al Garni SE, Abolaban F (2022) Electrical and dielectric properties of the natural calcite and quartz. Silicon 14(10):5265–5276. https://doi.org/10.1007/s12633-021-01318-7
53. Kumar K, Ravi M, Pavani Y, Bhavani S, Sharma A, VVR NR (2012) Electrical conduction mechanism in NaCl complexed PEO/PVP polymer blend electrolytes. J Non·Cryst Solids 358(23):3205–3211
54. Alsulami QA, Rajeh A (2021) Synthesis of the SWCNTs/TiO_2 nanostructure and its effect study on the thermal, optical, and conductivity properties of the CMC/PEO blend. Results Phys 28:104675
55. Gabal MA, Al-Harthy EA, Al Angari YM, Abdel Salam M, Awad A, Al-Juaid AA, Saeed A (2022) Synthesis, characterization and dye removal capability of conducting polypyrrole/$Mn_{0.8}Zn_{0.2}Fe_2O_4$/graphite oxide ternary composites. Catalysts 12(12):1624. https://doi.org/10.3390/catal12121624
56. Choudhary S, Sengwa R (2019) Investigation on structural and dielectric properties of silica nanoparticles incorporated poly (ethylene oxide)/poly (vinyl pyrrolidone) blend matrix based nanocomposites. J Inorg Organomet Polym Mater 29(2):592–607
57. Alwafi R, Saeed A (2022) Single-walled carbon nanotubes in nanosized basalts as nanocomposites: the electrical/dielectric properties and electromagnetic interference shielding performance. J Inorg Organomet Polym Mater 32(11):4340–4358. https://doi.org/10.1007/s10904-022-02450-6
58. Al-Muntaser AA, Pashameah RA, Sharma K, Alzahrani E, Tarabiah AE (2022) Reinforcement of structural, optical, electrical, and dielectric characteristics of CMC/PVA based on GNP/ZnO hybrid nanofiller: nanocomposites materials for energy-storage applications. Int J Energy Res 46(15):23984–23995
59. Choudhary S (2017) Dielectric dispersion and relaxations in (PVA-PEO)-ZnO polymer nanocomposites. Phys B: Condens Matter 522:48–56
60. Al-Muntaser A, AlSaidi RA, Sharma K, Alamri HR, Makhlouf M (2022) Structural, optical, electrical, and DFT studies on polyvinyl pyrrolidone/polyethylene oxide polymer blend filled with MoO3

nanoplates for flexible energy-storage devices. Int J Energy Res 46(10):13832–13843
61. Al-Muntaser A, Alzahrani E, Saeed A, Al Naim AF, Abo-Dief HM, Qusti SY, Tarabiah A (2023) An insight into the role of titanium oxide nanofiller on the structural, optical, electrical, and dielectric characteristics of PS/PVK composite. Phys Scr 98 (7)
62. Kaur S, Kumar A, Sharma AL, Singh DP (2019) Dielectric and energy storage behavior of CaCu3Ti4O12 nanoparticles for capacitor application. Ceram Int 45(6):7743–7747. https://doi.org/10.1016/j.ceramint.2019.01.077
63. Kaur S, Singh DP (2020) On the structural, dielectric and energy storage behaviour of PVDF- CaCu3Ti4O12 nanocomposite films. Mater Chem Phys 239:122301. https://doi.org/10.1016/j.matchemphys.2019.122301
64. Jaidka S, Aggarwal A, Chopra S, Singh DP (2022) Significantly enhanced dielectric behavior of polyvinylidene fluoride-barium strontium titanate flexible nanocomposite thick films: role of electric field-induced effects. J Electron Mater 51(9):5429–5439. https://doi.org/10.1007/s11664-022-09784-4
65. Koduru H, Scarpelli F, Marinov Y, Hadjichristov G, Rafailov P, Miloushev I, Petrov A, Godbert N, Bruno L, Scaramuzza N (2018) Characterization of PEO/PVP/GO nanocomposite solid polymer electrolyte membranes: microstructural, thermo-mechanical, and conductivity properties. Ionics 24(11):3459–3473
66. Al-Muntaser AA, Pashameah RA, Sharma K, Alzahrani E, Tarabiah AE (2022) Reinforcement of structural, optical, electrical, and dielectric characteristics of CMC/PVA based on GNP/ZnO hybrid nanofiller: nanocomposites materials for energy-storage applications. Int J Energy Res 46:23984–23995
67. Chérif SF, Chérif A, Dridi W, Zid MF (2020) Ac conductivity, electric modulus analysis, dielectric behavior and Bond Valence Sum analysis of Na3Nb4As3O19 compound. Arab J Chem 13(6):5627–5638. https://doi.org/10.1016/j.arabjc.2020.04.003
68. Chatterjee B, Gupta PN (2012) Nanocomposite films dispersed with silica nanoparticles extracted from earthworm humus. J Non·Cryst Solids 358(23):3355–3364. https://doi.org/10.1016/j.jnoncrysol.2012.08.020
69. Farea M, Abdelghany A, Oraby A (2020) Optical and dielectric characteristics of polyethylene oxide/sodium alginate-modified gold nanocomposites. RSC Adv 10(62):37621–37630
70. Youssif M, Abdelghany A, Abdelrazek E, Rashad D, Zidan H (2020) Structure dielectric correlation of PEO/PVP incorporated with biosynthesized gold nanoparticles. J Polym Res 27(12):1–14

Publisher's note Springer Nature remains neutral with regard to jurisdictional claims in published maps and institutional affiliations.

Affiliations

Mohammed M. Damoom[1,2] · Abdu Saeed[3,4] · Eida M. Alshammari[5] · Abdulsalam M. Alhawsawi[1,2] · A. Y. Yassin[6] · J. A. Mohammed Abdulwahed[7] · A. A. Al-Muntaser[8]

[1] Nuclear Engineering Department, King Abdulaziz University, Jeddah 21589, Saudi Arabia

[2] Center for Training & Radiation Protection, King Abdulaziz University, Jeddah 21589, Saudi Arabia

[3] Department of Physics, Faculty of Science, King Abdulaziz University, Jeddah 21589, Saudi Arabia

[4] Department of Physics, Thamar University, Thamar 87246, Yemen

[5] Department of Chemistry, College of Sciences, University of Ha'il, Ha'il 2440, Saudi Arabia

[6] Department of Basic Sciences, Delta University for Science & Technology, Gamassa, Egypt

[7] Physics Department, Umm Al-Qura University College in Qunfudah-Female, Mecca, Saudi Arabia

[8] Department of Physics, Faculty of Education and Applied Sciences at Arhab, Sana'a University, Sana'a, Yemen